

## MODELLING FLOW OVER A BACKWARD-FACING STEP USING THE F.E.M. AND THE TWO-EQUATION MODEL OF TURBULENCE

C. TAYLOR, C. E. THOMAS AND K. MORGAN

*Department of Civil Engineering, University College of Swansea, U.K.*

### SUMMARY

Flow over a downstream-facing step is predicted using the F.E.M. A two-equation model of turbulence is employed where the transport of turbulence kinetic energy and dissipation rate are depicted using transport-type equations, i.e. the two-equation model of turbulence. The results obtained are compared with other models and experimental results. Generally, the model was found to be under-predictive with regard to the reattachment length when previous empirical data was used in the transport equations.

KEY WORDS Numerical Methods Turbulence Separation

### INTRODUCTION

An accurate simulation of separated flow is of particular importance when designing pipe networks, hydraulic control systems, channels and diffusers. In each, the local variation in velocity and energy is of significance in the predicted operation of the overall system. The present work is directed at the utilization of the finite element method (F.E.M.) to solve one such problem—turbulent flow over a downstream-facing step, Figure 1. The flow is considered to be two-dimensional, steady, incompressible and is analysed utilizing the two-equation model of turbulence.<sup>1</sup>

During recent years the F.E.M. has been employed quite extensively in predicting both laminar<sup>2-6</sup> and turbulent<sup>7-14</sup> flow. The technique now complements other methods for solving problems where the flow is governed by the generalized Navier–Stokes equations and has become a useful addition to the scientists' repertoire of methods for solving such problems.

The present paper is an extension of the previous work by the authors<sup>13</sup> when the one-equation model was used to predict turbulent flow over a downstream-facing step. The fluid motion is assumed to be governed by the Navier–Stokes equations, the equation of continuity, a turbulence transport equation and an equation depicting local dissipation. The F.E.M. is used to effect a spatial discretization and variation in the primitive variables and the resulting discrete form of the governing equations is then solved, iteratively, in order to ascertain the spatial variation in the pertinent variables. The resulting solutions obtained are compared with known experimental<sup>15</sup> and numerical<sup>16</sup> results.

### THEORETICAL FORMULATION

The region of interest is shown, diagrammatically, on Figure 1, and consists of a single backward-facing step in a channel. The flow is two-dimensional, steady and both the laminar

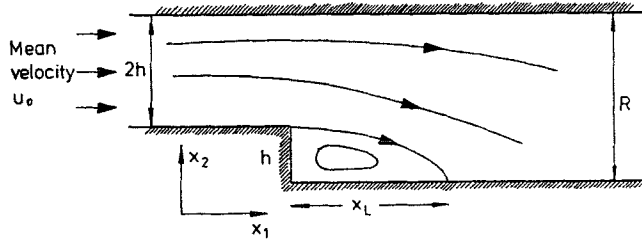


Figure 1

viscosity and density are assumed to be constant; the walls are smooth and impermeable.

A set of differential equations which are commonly used to depict the flow under the prescribed conditions are,

$$\rho u_i \frac{\partial u_i}{\partial x_j} = -\frac{\partial p}{\partial x_i} + \frac{\partial}{\partial x_j} \left[ \mu_e \left( \frac{\partial u_i}{\partial x_j} + \frac{\partial u_j}{\partial x_i} \right) \right] \quad (1)$$

and

$$\rho \frac{\partial u_i}{\partial x_i} = 0 \quad (2)$$

in which  $u_i$  denotes the velocity vector in the  $i$ th co-ordinate direction,  $p$  the local pressure,  $\rho$  the density and  $\mu_e$  the effective viscosity. All variables are time-averaged and the effective viscosity is written

$$\mu_e = \mu + \mu_t \quad (3)$$

where  $\mu$  is the laminar viscosity and  $\mu_t$  the turbulent viscosity whose value varies pointwise throughout the flow domain. The magnitude of the turbulent viscosity can be defined<sup>17,18</sup> in terms of the turbulence kinetic energy,  $k$ , and  $l$ , the turbulent length scale, and a constant  $C_\mu$ ,

$$\mu_t = C_\mu \rho k^{1/2} l \quad (4)$$

The present text is concerned with the evaluation of both  $k$  and  $l$  from two further transport equations. These are,

$$\rho u_j \frac{\partial k}{\partial x_j} = \frac{\partial}{\partial x_j} \left[ \left( \mu + \frac{\mu_t}{\sigma_k} \right) \frac{\partial k}{\partial x_j} \right] + \mu_t \frac{\partial u_i}{\partial x_j} \left( \frac{\partial u_i}{\partial x_j} + \frac{\partial u_j}{\partial x_i} \right) - C_D \rho k^{3/2} / l \quad (5)$$

for the turbulence kinetic energy and,

$$\rho u_j \frac{\partial \epsilon}{\partial x_j} = \frac{\partial}{\partial x_j} \left[ \left( \mu + \frac{\mu_t}{\sigma_\epsilon} \right) \frac{\partial \epsilon}{\partial x_j} \right] + C_1 \rho k \frac{\partial u_i}{\partial x_j} \left( \frac{\partial u_i}{\partial x_j} + \frac{\partial u_j}{\partial x_i} \right) - C_2 \rho \frac{\epsilon^2}{k} \quad (6)$$

where,  $\sigma_k$ ,  $\sigma_\epsilon$ ,  $C_D$ ,  $C_1$  and  $C_2$  are usually considered to be constant,<sup>1</sup> and  $\epsilon = k^{3/2}/l$ . A comprehensive investigation regarding the evaluation of the above constants has been presented<sup>19</sup> in which the values are given as,

$$C_\mu = 0.22, C_D = 0.092, \sigma_k = 1.00, \sigma_\epsilon = 1.3, C_1 = 1.45 \text{ and } C_2 = 0.18$$

These values are based on a rational investigation of the basic equations in the near-wall region and the incorporation of observations from experimental investigators.<sup>20</sup> This, combined with the so-called computer optimization techniques,<sup>21</sup> results in the values given above.

BOUNDARY CONDITIONS

*Upstream*

Boundary conditions were imposed at a distance of 3 1/3 step lengths upstream from the step. Two sets were tried,

(i) those imposed during the solution of the one-equation model,<sup>13</sup>

$u_1$ —specified } experimental inlet profiles  
 $u_2=0$  } of Denham *et al.*<sup>15</sup>  
 $k$ —specified }  $x_1 = 0, 0 < x_2 < R$   
 $l$ —those used for the one-equation model  
 $\epsilon$ —calculated from  $k^{3/2}/l$ .

and

(ii) the values obtained for fully developed flow in a uniform channel equal in width to that upstream of the step. For this analysis the boundary conditions cited in (i) above were used at the upstream end of the channel with downstream conditions of

$$\left. \begin{array}{l} \frac{\partial u_1}{\partial x_1} = 0 \\ u_2 = 0 \\ \frac{\partial k}{\partial x_1} = 0 \\ p = 0 \end{array} \right\} 0 < x_2 < R$$

The upstream boundary conditions imposed when analysing flow over the step are, therefore,

$u_1$ —specified } from fully developed two-equation model analysis  
 $u_2=0$  } on straight channel  
 $k$ —specified }  
 $l$ —fully developed values of the one-equation model  
 $\epsilon$ —fully developed values of the one-equation model

It was found that some variation in the velocity and the  $k, \epsilon$  distribution was apparent depending on which upstream boundary condition was utilized, the better distribution being obtained when the second type is imposed.

*Downstream*

These are compatible with fully developed flow,

$$\left. \begin{array}{l} \frac{\partial u_1}{\partial x_1} = 0 \\ \frac{\partial u_2}{\partial x_1} = 0 \\ \frac{\partial k}{\partial x_1} = 0 \end{array} \right\} 0 < x_2 < R$$

$l$ —fully developed values from a one-equation model

$$\epsilon = \frac{k^{3/2}}{l}$$

$$p = 0$$

Wall

If the walls are smooth, rigid, impermeable and the no-slip condition is valid then all variables assume a zero value at the wall. However, the variation in such quantities quite close to the wall renders the imposition of zero values impractical unless a very fine mesh discretization is used near the wall or special elements are employed.<sup>8,21</sup> Indeed, such refinement could lead to excessive core and c.p.u. requirements and is usually discarded.

A generally accepted technique which obviates the necessity to follow rapid near-wall variations is to terminate the mesh at some distance away from the wall, and utilize the universal laws depicting the variation in shear velocity in the near wall region.<sup>22</sup>

$$\left. \begin{aligned} u_i^* &= \lambda^* & 0 \leq \lambda^* \leq 5 \\ u_i^* &= (-3.05 + 5.0 \log \lambda^*) \left( \frac{\tau_w}{|\tau_w|} \right) & 5 \leq \lambda^* \leq 30 \\ u_i^* &= (-5.5 + 2.5 \log \lambda^*) \left( \frac{\tau_w}{|\tau_w|} \right) & \lambda^* > 30 \end{aligned} \right\} \quad (7)$$

in which

$$u_i^* = u_i / \sqrt{\left| \frac{\tau_w}{\rho} \right|}; \quad \lambda^* = \left( \frac{\lambda}{\mu} \right) \sqrt{\left| \frac{\tau_w}{\rho} \right|} \quad (8)$$

$i = 1$  for boundaries parallel to the  $u_1$ -axis

$i = 2$  for boundaries parallel to the  $u_2$ -axis

$\lambda$  = distance measured normal from wall

The shear stress at the limit of the near-wall region is assumed to be identical with that at the wall,  $\tau_w = \mu(\partial u_i / \partial \lambda)$ . Once the gradient in velocity and associated shear stress can be evaluated then the near-wall value of  $k$  can be calculated from

$$k = \frac{|\tau_w|}{C_D^{1/2} \rho} \quad (9)$$

where the absolute magnitude for  $\tau_w$  is included since  $k$  must always be positive. This is derived from the usual assumption that the variation in static pressure normal to a wall can be ignored and derivatives of the pertinent variables parallel to the wall are small compared to those normal to the wall. Using these assumptions (9) becomes a particular solution of the generalized equation depicting transport  $k$ , provided that the location under consideration is within the fully turbulent region.

The near-wall values of  $\epsilon$  may now be found if the length scale is defined. Following the procedure adopted for the one-equation model with  $l = \lambda$ , the values of  $\epsilon$  can be defined since

$$\epsilon = \frac{k^{3/2}}{l} \quad (10)$$

Since the discretized domain terminates at some small distance away from the wall the above conditions will also apply at the upstream and downstream extremities of the domain.

METHOD OF SOLUTION

Quadrilateral isoparametric elements are used and the now standard approach to equation formulation into matrix form is adopted.<sup>23</sup> The resulting matrix equation can be written in a generalized form,

$$\mathbf{H}\boldsymbol{\beta} = \mathbf{f} \tag{11}$$

in which the matrix  $\mathbf{H}$  is non-symmetric. Details of the coefficients of  $\mathbf{H}$  and composition of  $\mathbf{f}$  are as presented in Reference 14. The only additional equation to be incorporated is (6) which can either be included in  $\mathbf{H}$  in exactly the same manner as (5) leading to a single matrix where,

$$\boldsymbol{\beta}^k = \begin{Bmatrix} u_1^k \\ p^k \\ u_2^k \\ k^k \\ \epsilon^k \end{Bmatrix} \text{ for a corner node}$$

and

$$\boldsymbol{\beta}^k = \begin{Bmatrix} u_1^k \\ u_2^k \\ k^k \\ \epsilon^k \end{Bmatrix} \text{ for a mid-side node.}$$

Alternatively (6) can be omitted from  $\mathbf{H}$  and once the other variables have been found, a separate calculation is undertaken to find the distribution of the matrix resulting from a separate F.E. formulation.<sup>14</sup> Whichever solution technique is adopted, the required distribution of stream function can be evaluated from,

$$\nabla^2\psi = \frac{\partial u}{\partial y} - \frac{\partial v}{\partial x}$$

again employing the F.E.M.

ITERATIVE TECHNIQUE

As indicated above, two schemes were adopted. In the first, the discretized equation is incorporated into the global matrix  $\mathbf{H}$ . Initial values over the whole domain corresponded to those obtained from a one-equation model solution and the near-wall boundary values calculated accordingly. Although this technique proved to be quite amenable to solution, the computer core requirements were excessive and placed a limitation on the fineness of the mesh that could be accommodated. The alternative approach was then adopted where the  $\epsilon$  equation was uncoupled and solved in isolation. The corresponding iteration scheme is

- (i) Set all initial values to zero within the flow domain and assume that the effective viscosity corresponds to the molecular viscosity,
- (ii) Solve for  $u$ ,  $p$  and  $k$  for a fixed distribution of  $l$  (3 iterations on 1st entry to problem),
- (iii) Estimate near-wall and inlet boundary conditions for  $\epsilon$  using  $\epsilon = C_\mu(k^{3/2}/l)$

- (iv) Solve the  $\epsilon$  equation using fixed values of  $u_i$ ,  $p$  and  $k$ ,
- (v) Test on convergence of  $\epsilon$ ; if not converged go to (iii),
- (vi) Update  $l$  using  $l = C_\mu(k^{3/2}/\epsilon)$ ,
- (vii) Update  $\mu_t$  using the new  $k$  and  $l$  values,
- (viii) Using equation (8) re-estimate the wall shear stress and therefore the boundary conditions on  $u_i$  and  $k$ ,
- (ix) Repeat from (ii) until convergence criteria satisfied.

It was found, during the application of the above iterative technique that (v) would initiate several iterations for  $\epsilon$  for set values of the remaining variables. This would sometimes cause divergence since the distribution is highly sensitive to variations in either the upstream or downstream boundary conditions. Far better stability and distribution was obtained when fully developed values on  $u_i$ ,  $k$  and  $P$  were imposed upstream and a corresponding ( $\partial\epsilon/\partial x_1 = 0$  downstream) as opposed to  $\epsilon = C_\mu(k^{3/2}/l)$ . Relaxation factors were optimized, for the mesh used, Figure 2, to an under-relaxation factor, on all variables, except  $\mu_t$ , of 0.8 and a corresponding factor of 0.5 on  $\mu_t$ . If negative values of  $k$  and  $\epsilon$  emerged after a particular iteration,  $k$  was set to a small +ve value and if  $\epsilon$  persisted to be -ve then an  $l_n$  set to  $\frac{1}{2}(l_{n-1} + l_{n+1})$  would usually overcome this difficulty. These restrictions led to converged solutions being obtained without a great deal of difficulty and did not violate the physical behaviour of the variables.

### NUMERICAL CALCULATIONS

The spatial discretization used for the present calculations is shown on Figure 2. This mesh proved adequate for present purposes and local refinements did not result in an appreciable increase in accuracy.

During numerical calculations the initial values were taken as zero throughout the domain although special care was exercised when imposing boundary conditions. The upstream boundary conditions were evaluated by conducting an analysis of flow in a channel equal in width to that upstream of the step. The one-equation model boundary conditions were imposed upstream and the flow allowed to develop to a fully developed profile downstream. The mesh used and boundary conditions imposed are shown on Figure 3. The fully developed values of velocity and  $k$  were then employed as upstream boundary conditions for the step problem. Gradients of all variables, except pressure, were taken as zero on the downstream face, again implying fully developed conditions. It was found, however, during trial calculations, that the imposition of boundary conditions on  $\epsilon$  on other than fully

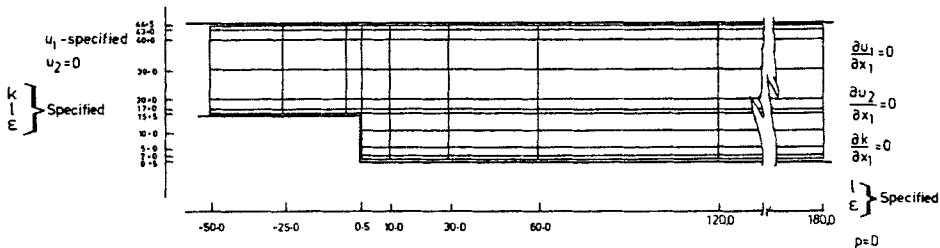


Figure 2. Mesh for backward-facing step

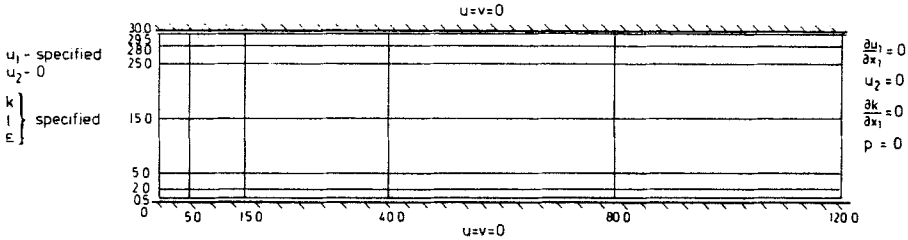


Figure 3. Straight channel mesh and boundary conditions

developed values on the upstream boundary did not change the results to any marked degree. The values of this variable seemed to develop to essentially the same values at the step irrespective of small changes in  $\epsilon$  on the upstream boundary.

The first problem analysed corresponds to a Reynolds number of 3025 which corresponds to that taken by Atkins.<sup>19</sup> These are compared on Figure 4 which also includes the experimental results of Denham *et al.*<sup>15</sup> The one-equation model results obtained using the F.E.M.<sup>13</sup> are also shown for comparison purposes, Figure 5. Contour plots showing the overall distribution of  $k$  are shown on Figure 6 and plots for stream functions on Figures 7 and 8. For  $Re=3025$ , the one-equation model takes 30 iterations to converge; the two-equation model takes 125 iterations.

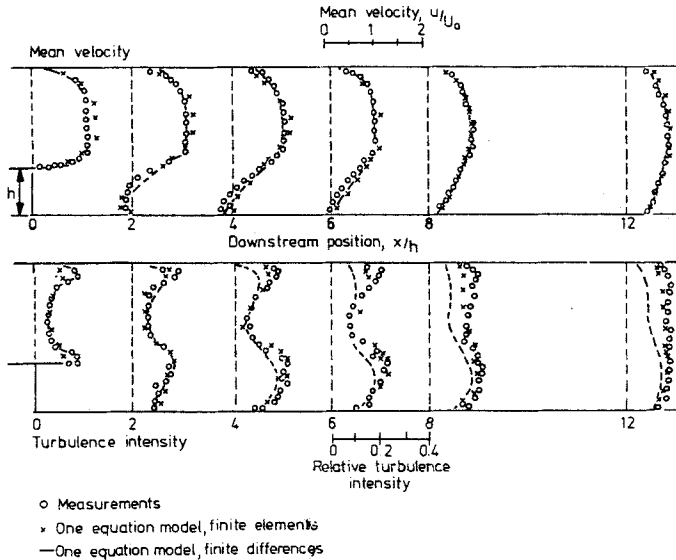


Figure 4. Velocity and turbulence intensity plots for  $Re = 3025$ —one-equation model

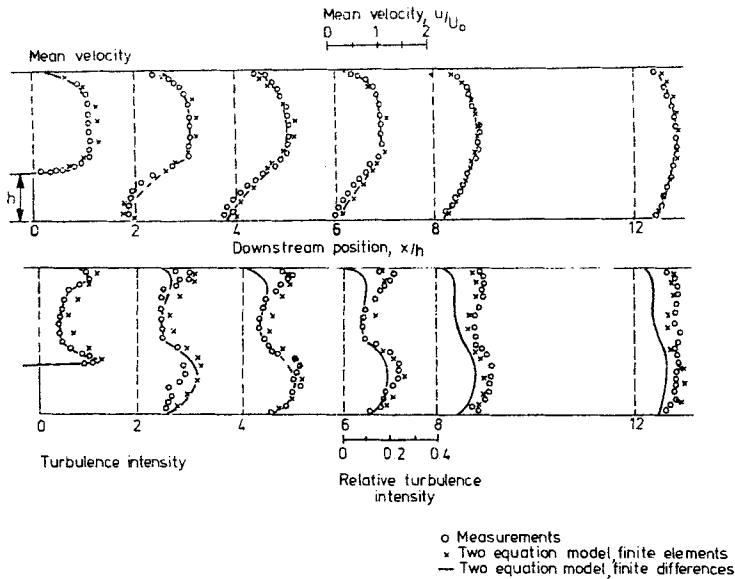


Figure 5. Velocity and turbulence intensity plots for  $Re = 3025$ —two-equation model

## CONCLUSIONS

In general the F.E.M. has been demonstrated to be a viable technique for the prediction of turbulent flow over a backward-facing step. There are, however, some discernible differences between the calculated values from the one- and two-equation models. In the first instance, the recirculation zone length was found to be rather less than  $4.5h$  as opposed to  $5.6h$  for the one-equation model. These are both somewhat lower than the experimental value<sup>15</sup> of approximately  $6h$ , although slightly better than the values obtained utilizing the finite difference technique,<sup>16</sup>  $4.2h$  and  $5.2h$ . Secondly, a better distribution of turbulence kinetic energy was obtained using the one-equation model. This is apparent from Figures 4 and 5. This, associated with the fact that  $\sigma_k = 1.53$  had to be incorporated in both the F.E. and finite difference methods as opposed to  $\sigma_k = 1.00$ ,<sup>16</sup> seems to indicate that no advantage has been gained whilst the complexity of the calculations has been increased.

Two points emerge when comparing the present two-equation model results with the previously published finite difference solutions. The first is that the correlation between measured and calculated velocity distribution is quite good. This is in spite of the fact that the upstream boundary conditions are slightly different. This enhances the observations made by previous researchers.<sup>16</sup> The second fact is that the correlation, with respect to  $k$ , between experiment and the F.E.M. is significantly better than those published using finite difference calculations.



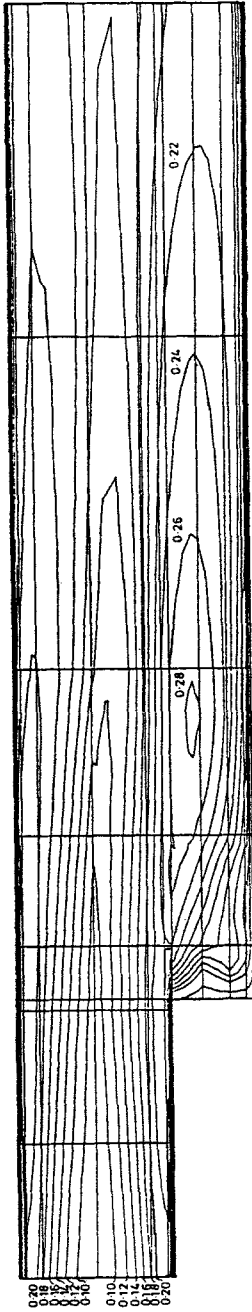


Figure 6. Contour plots of turbulent kinetic energy

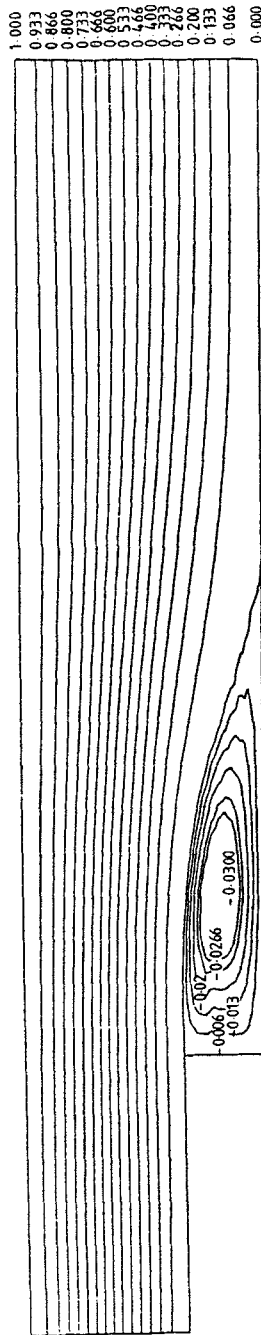


Figure 7. Streamline plots for the one-equation model (Re = 3025)

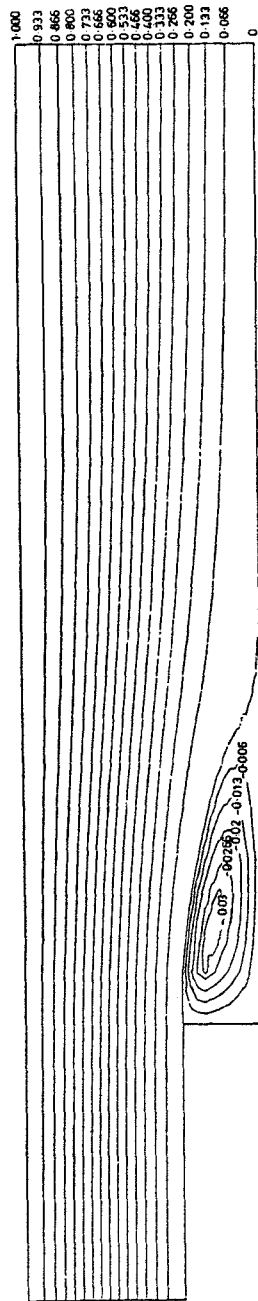


Figure 8. Streamline plot for the two-equation model (Re = 3025)

## REFERENCES

1. B. E. Launder and D. B. Spalding, *Mathematical Models of Turbulence*, Academic Press, London/New York, 1972.
2. J. T. Oden, *Finite Elements of Non-Linear Continua*, McGraw-Hill, 1972.
3. C. Taylor and P. Hood, 'A numerical solution of the Navier-Stokes equations using the Finite Element Technique', *Int. J. Comp. and Fluids*, **1**, 73-100 (1973).
4. C. Taylor and P. Hood, 'Navier-Stokes equations using mixed interpolation', *Proc. Int. Conf. on F.E.M. in Flow Problems*, Swansea, pp. 121-132 (1974).
5. T. J. R. Hughes, R. L. Taylor and J. F. Levy, 'A finite element method for incompressible viscous flows', *Proc. 2nd Int. Conf. on F.E.M. in Flow Problems*, Rapallo, Italy, pp. 1-16 (1976).
6. R. M. Smith, 'A study of laminar flow entrance sections using the F.E.M.', *C.E.G.B. Report No. RD/B/M3513* (1975).
7. R. Gerrard, 'Finite element solution of flow in non-circular conduits', *Proc. A.S.C.E., J. Hyd. Div.*, **100**, HY3, 425-441 (1974).
8. C. Taylor, T. G. Hughes and K. Morgan, 'A numerical analysis of turbulent flow in pipes', *Int. J. Comp. and Fluids*, **5**, 191-204 (1977).
9. K. Morgan, T. G. Hughes and C. Taylor, 'A numerical model of turbulent shear flow behind a prolate spheroid', *Applied Math. Modelling*, **2**, 271-274 (1978).
10. A. J. Baker, 'Finite element analysis of turbulent flows', *Proc. 1st Int. Conf. Num. Meth. in Turbulent Flows*, Swansea, pp. 203-229 (1978).
11. C. Taylor, T. G. Hughes and K. Morgan, 'Finite element solution of one-equation models of turbulent flow', *J. Comp. Phys.*, **29**, 163-172 (1978).
12. K. Morgan, T. G. Hughes and C. Taylor, 'The analysis of turbulent free shear flows by the F.E.M.', *Comp. Meth. in Appl. Mech. and Eng.*, **19**, 117-125 (1979).
13. C. E. Thomas, K. Morgan and C. Taylor, 'Finite element analysis of flow over a backward facing step', *Comp. and Fluids*, **9**, 265-278 (1981).
14. C. Taylor, T. G. Hughes and K. Morgan, 'A finite element model of one and two equation models of turbulent flow', *Recent Advances in Num. Meth. in Fluids*, **1**, Pineridge Press, 311-334 (1980).
15. M. K. Denham, P. Briard and M. A. Patrick, 'A directionally sensitive laser anemometer for velocity measurements in highly turbulent flow', *J. Physic E: Scientific Instruments*, **8**, 681-683 (1975).
16. D. J. Atkins, S. J. Maskell and M. A. Patrick, 'Numerical prediction of separated flows', *Int. J. num. Meth. Engng*, **15**, 129-144 (1980).
17. L. Prandtl, 'Über ein neues Formelsystem für die ausgebildete Turbulenz', *Nachr. Akad. der Wissenschaft in Göttingen*, 1945.
18. A. N. Kolmogorov, 'Equations of turbulent motion of an incompressible fluid', *FZV. Akad. Nauk. SSSR Ser. Phys.* **VI**, 1-2, 56-58 (1942).
19. D. J. Atkins, 'Numerical studies of separated flows', *Ph.D. Thesis*, Exeter University, 1974.
20. J. Laufer, 'The structure of turbulence in fully-developed pipe flow' *NACA Rep. 1174* (1953).
21. A. G. Hutton and R. M. Smith, 'The prediction of laminar flow over a downstream facing step', *C.E.G.B. Rep. RD/B/N3660* (1979).
22. J. T. Davies, *Turbulence Phenomena*, Academic Press, New York, 1972.
23. C. Taylor and T. G. Hughes, *Finite Element Programming of the Navier-Stokes Equations*, Pineridge Press, 1981.